CERES_FluxByCldTyp-Day/Month_Ed4A
Data Quality Summary

Version 2
Updated 2/8/2022

Investigation: **CERES**
Data Products: **FluxByCldTyp-Day/Month**

Data Sets: **Terra+Aqua**

Data Set Versions: **Terra+Aqua Edition4A** **Release Date: May 28, 2020**

CERES Visualization, Ordering and Subsetting Tool: https://ceres.larc.nasa.gov/data/

The purpose of this document is to inform users of the accuracy of this data product as determined by the CERES Science Team. The document summarizes key validation results, provides cautions where users might easily misinterpret the data, provides links to further information about the data product, algorithms, and accuracy, and gives information about planned data improvements.

This document is a high-level summary and represents the minimum information needed by scientists for appropriate and successful use of this data product. It is strongly suggested that authors, researchers, and reviewers of research papers re-check this document (especially Cautions and Helpful Hints) for the latest status before publication of any scientific papers using this data product.

Important Note to Users:
FluxByCldTyp-Day/Month Ed4A product is the initial release of this product. Users are encouraged to provide the CERES science team any suggestions to improve or to increase the usability of this product by emailing LaRC-CERES-Help@mail.nasa.gov.

Important Update to Note as of April 14, 2021:
***Please see the RED bullet in* Cautions and Helpful Hints.**

TABLE OF CONTENTS

Section Page

LIST OF FIGURES

Figure Page

LIST OF FIGURES

Figure Page

LIST OF TABLES

Table Page

1.0 Nature of the CERES_FluxByCldTyp_Day/Month_Ed4A Products

The CERES FluxByCldTyp-Day/Month Ed4A products provide Terra and Aqua daytime 1°-regional gridded daily and monthly averaged top of the atmosphere (TOA) radiative fluxes and associated MODIS-derived cloud properties stratified by cloud optical depth and cloud effective pressure. This is the initial release of the FluxByCldTyp-Day/Month product. TOA longwave (LW) and shortwave (SW) fluxes are provided for 42 cloud types demarcated by 6 cloud optical depth and 7 cloud effective pressure layer bins (see Figure 1-1) as well as for the observed all-sky and clear-sky conditions. The mean cloud amount, cloud effective pressure, effective temperature, particle radius, liquid water path/ice water path (LWP/IWP), infrared (IR) emissivity, and optical depth are provided for each of the 42 cloud types and for the combined 42 cloud types (or total cloud conditions). The incoming solar daily irradiance is from the SORCE TSI [Solar Radiation and Climate Experiment, Total Solar Irradiance, (Kopp et al. 2005)]. Although there are two CERES instruments on both Terra and Aqua, only the instrument in cross-track mode is utilized.

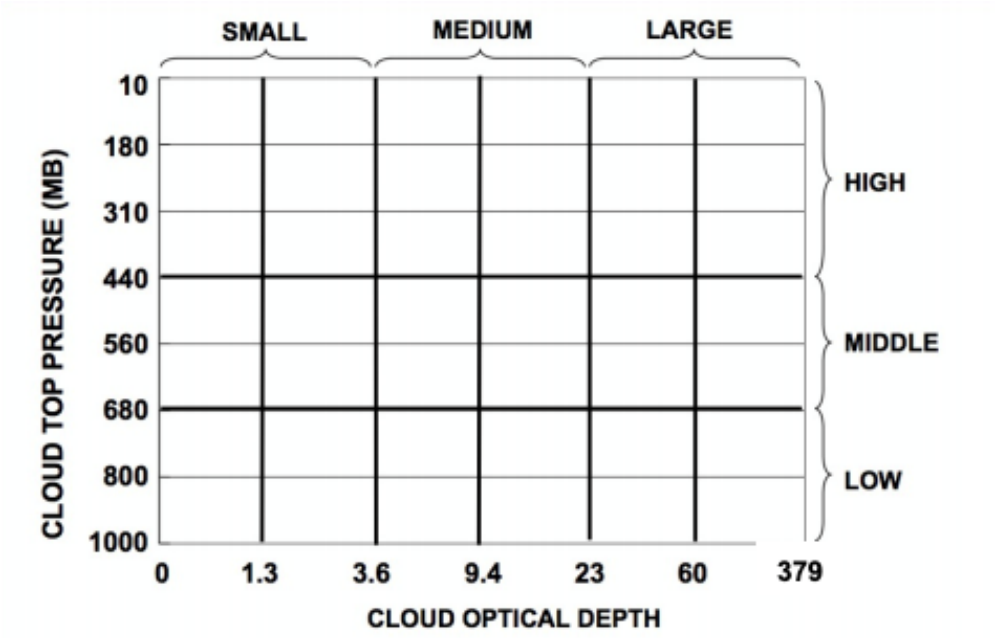

Figure 1-1. The CERES FluxByCldTyp 42 cloud types classified by cloud optical depth and cloud effective pressure. Note it is the same classification that ISCCP employs.

The daytime FluxByCldTyp fluxes and clouds are based on CERES SSF Ed4A measurements that have a solar zenith angle (SZA) less than 82°. The CERES MODIS cloud retrievals are based on three algorithms depending on the observed SZA. For SZA<82° the cloud retrieval incorporates both visible and IR channels, for SZA>90° only IR channels are utilized, and for twilight the daytime retrieval algorithm is modified to handle near-terminator solar conditions. The nighttime optical depth maximum range is limited, since IR channels saturate at an optical depth of ~6,

whereas the daytime optical depths are derived from visible channels having optical depths up to ~150. Since consistent 24-hour cloud-type identification is not possible, the FluxByCldTyp only utilizes daytime observations to ensure consistency. The FluxByCldTyp product does not provide a true 24-hour averaged LW flux, but simply an average of all the daytime Terra and Aqua observed LW fluxes. No nighttime LW flux measurements are used. The FluxByCldTyp regional SW 24-hour fluxes are based on diurnal albedo models that are dependent on the measured cloud properties, which are assumed to be invariant over the day. The number of SW and LW cloudy-sky and clear-sky observations are provided in the product to allow the user to assess the sampling robustness.

The CERES SSF Ed4A product Terra and Aqua nominal 20-km footprints are sub-divided into clear-sky and two dynamic cloud layer areas based on the associated MODIS pixel-level clouds (Figure 1-2). MODIS-derived broadband (BB) radiances are computed for each of the sub-footprint areas based on MODIS narrowband (NB) radiances. Both the SW and LW MODIS narrowband to broadband conversion coefficients were empirically derived from homogeneous (single scene type) footprint MODIS and CERES radiances. Then the sub-footprint derived BB radiances are converted to fluxes by employing the CERES Ed4A Angular Distribution Models (ADMs), which are used to convert the CERES SSF footprint observed radiances into fluxes. The sub-footprint BB fluxes are weighted by their area fraction to compute footprint flux. The footprint flux is then compared to CERES observed flux in order to normalize the sub-footprint fluxes to the CERES observed footprint flux. The sub-footprint flux is then assigned to a cloud type according to the mean imager cloud optical depth and effective pressure as demarcated in Figure 1-1.

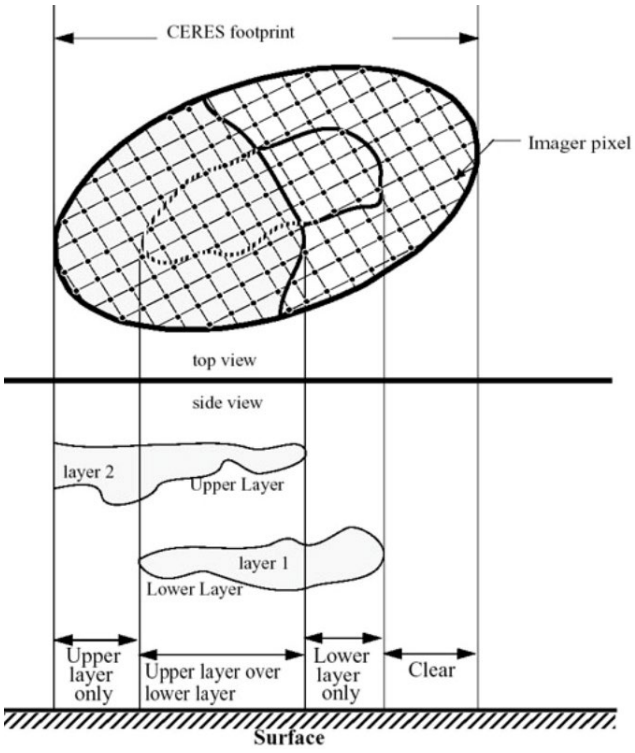

Figure 1-2. A schematic that illustrates the two cloud layers and clear-sky areas of the CERES 20-km nominal footprint. The imager pixels define the cloud properties of the layer as well as provide the channel radiances needed to compute BB radiance at the sub-footprint scale. Note that the upper layer cloud may include lower layer clouds not seen by the satellite. Both the single layer and multi-layer portions of the upper-level cloud are considered as the upper layer cloud.

The instantaneous sub-footprint fluxes and their associated MODIS cloud properties are gridded into 1° regions. The center latitude and longitude of the CERES footprint assigns the region. Sub-footprint fluxes with the same cloud type are averaged by fraction weighting. The regional cloud-type fraction is the sum of the sub-footprint fractions divided by the total number of footprints located in the region. The regional all-sky flux is the fraction-weighted mean of all the cloud-type and clear-sky fluxes. The instantaneous regional sum of all the cloud-type and clear-sky fractions should equal 1.0.

All of the Terra and Aqua instantaneous observed regional cloud-type fluxes over the day are averaged by their respective cloud-type fractions. The daily LW fluxes contained in the FluxByCldTyp product do not represent a 24-hour averaged LW flux, since no twilight or nighttime flux measurements are utilized. This is especially true over land, where the near local noon daytime Terra and Aqua measurements observe the peak of the land diurnal temperature cycle. In contrast, the CERES SSF1deg-Day/Month LW fluxes are based on temporal interpolation in between the daytime and nighttime measurements to more accurately estimate the regional diurnal flux.

Instantaneous SW fluxes cannot simply be averaged, since the SW flux is a function of the observed solar zenith angle. The SW flux measurements are normalized by computing an *equivalent* daily SW flux assuming that the cloud conditions observed at the time of the measurement persist over the day. These diurnal albedo models are based upon the CERES Angular Distribution Models (ADMs) developed for the Tropical Rainfall Measuring Mission (TRMM) satellite (Loeb et al. 2003). The TRMM satellite precessed across all solar zenith angles observed in the tropics. The Terra and Aqua sun-synchronous orbits are maintained at a 10:30 and 1:30 local equator crossing time and observe only a limited range of regional solar zenith angles. These diurnal albedo models are symmetric about local noon. All of the daytime observed Terra and Aqua *equivalent* daily mean SW fluxes are then averaged by cloud type. The combination of Terra and Aqua measurements captures most of the regional diurnal cycle except for regions of early morning maritime stratus and late afternoon convection over land.

The monthly mean cloud-type fluxes are determined from the daily fluxes as follows. The FluxByCldTyp day and month products are GMT-based. This facilitates comparisons with climate models, unlike local time based products. For regions near Greenwich, the local and GMT days are similar, however, for regions near the west side of the dateline (170°E) the afternoon of the previous local day and the morning of the following local day are combined with local midnight occurring during the middle of the GMT day. The monthly regional cloud-type fraction is the sum of the daily cloud-type fractions divided by the number of days in the month. The monthly cloud-type LW flux is computed from the daily LW fluxes weighted by their associated cloud-type fractions. Rather than computing the monthly mean SW flux by directly averaging the daily measurements, we compute the monthly mean cloud-type SW flux by multiplying the monthly solar incoming flux by the monthly mean albedo, mitigating the bias incurred by the daily cloud-type sampling distribution while the regional daily solar incoming flux is changing day-to-day with solar zenith angle. The cloud-type monthly mean albedo is derived from the cloud-type fraction-weighted *equivalent* daily SW flux and daily incoming solar insolation for all the daily observations in a month.

For each cloud type, the cloud fraction, the cloud effective pressure and temperature, optical depth, and IR emissivity are provided in the FluxByCldTyp product. The liquid and ice cloud fractions, water paths and particle sizes are also provided. Cloud optical depth is averaged in logarithm form, since the logarithm of the cloud optical depth is proportional to the visible radiance. The total cloud properties are computed by the fraction weighting the individual cloud-type properties. The all-sky fluxes are computed from the cloud-type and clear-sky fluxes by weighting their associated fractions. The FluxByCldTyp daily product provides the total number of regional SW and LW cloudy and clear-sky flux Terra and Aqua measurements observed over the day. The FluxByCldTyp monthly product provides the total number of regional SW and LW cloudy and clear-sky flux measurements observed over the month and includes the number of days with measurements. The frequency statistics will allow the user to evaluate if there is sufficient cloud-type sampling to ensure a meaningful flux. The mean daily and monthly solar zenith angles are also provided.

We urge users to visit the CERES Data subsetting/visualization/ordering tool https://ceres.larc.nasa.gov/data/, which provides an user friendly interface and a wider range of data formats (e.g., ASCII, netCDF). The FluxByCldTyp-Day/Month products may also be ordered from https://asdc.larc.nasa.gov/project/CERES under Level 3.

2.0 CERES Processing Level and Product Description

This section explains the CERES processing flow from level 0 to level 3 products; the steps are summarized in Table 2-1. This section also briefly describes all of the publicly available CERES products and their processing differences to help the user find the appropriate product for their application.

Table 2-1. CERES processing level descriptions.

Level	Description	Data Product
0	Raw digitized instrument data for all engineering and science data streams in Consultative Committee for Space Data Systems (CCSDS) packet format.	
1B	Instantaneous filtered broadband radiances at the CERES footprint resolution, geolocation and viewing geometry, solar geometry, satellite position and velocity, and all raw engineering and instrument status data.	BiDirectional Scans (BDS)
2	Instantaneous geophysical variables at the CERES footprint resolution. Includes some Level 1B parameters and retrieved or computed geophysical variables (e.g., filtered and unfiltered radiances, viewing geometry, radiative fluxes, imager cloud and aerosol properties).	SSF
3	Radiative fluxes and cloud properties spatially averaged onto a uniform grid. Includes either instantaneous averages sorted by GMT hour or temporally interpolated averages at 1–hourly, daily, monthly or monthly hourly.	SSF1deg-Hour SSF1deg-Day, -Month SYN1deg-Hour, -Day, -MHour, -Month CldTypHist-Month, MHour FluxByCldTyp-Day, -Month
3B	Level 3 data products adjusted within their range of uncertainty to satisfy known constraints (e.g., consistency between average global net TOA flux imbalance and ocean heat storage).	EBAF-TOA EBAF

CERES instruments fly on the Terra (descending sun-synchronous orbit with an equator crossing time of 10:30 A.M. local time) and Aqua or NPP (ascending sun-synchronous orbit with an equator crossing time of 1:30 P.M. local time) satellites. Each CERES instrument measures filtered radiances in the shortwave (SW; wavelengths between 0.3 and 5 μm), total (TOT; wavelengths between 0.3 and 200 μm), and window (WN; wavelengths between 8 and 12 μm) regions. Unfiltered SW, longwave (LW) and WN radiances are determined following Loeb et al. (2001). CERES instruments provide global coverage daily, and monthly mean regional fluxes are based upon complete daily samples over the entire globe.

Raw digitized instrument data (Level 0) are converted to instantaneous filtered radiances (Level 1) using the latest CERES gains (Thomas et al. 2010). Time-dependent spectral response function values are then used to correct for the imperfect spectral response of the instrument and convert the filtered radiances into unfiltered SW, LW and WN radiances (Loeb et al. 2001; Loeb et al. 2016). Since there is no LW channel on CERES, LW daytime radiances are determined from the difference between the TOT and SW channel radiances. Instantaneous TOA radiative fluxes (Level 2) are estimated from unfiltered radiances using empirical ADMs (Su et al. 2015a) for different scene types identified using cloud property retrievals from MODIS measurements (Minnis et al. 2011). Their accuracy has been evaluated in several articles (Loeb et al. 2005 Loeb et al. 2007; Kato and Loeb 2005; Su et al. 2015b).

Monthly mean fluxes (Level 3) are determined by spatially averaging the instantaneous TOA flux values on a 1°×1° grid, temporally interpolating between observed values at 1-h increments for each hour of every month, and then averaging all hour boxes in a month (Doelling et al. 2013). CERES employs the CERES-only (CO; CERES SSF1deg stream) and the CERES-geostationary (CG; CERES SYN1deg stream) temporal interpolation methods. The CO method assumes that the cloud properties at the time of the CERES observation remain constant and only accounts for changes in albedo with solar zenith angle and diurnal land heating, by assuming a shape for unresolved changes in the diurnal cycle. The CG method enhances the CERES data by explicitly accounting for changes in clouds and radiation between CERES observation times using 1-hourly imager data from five geostationary (GEO) satellites that cover 60°S-60°N at any given time.

The Energy Balanced and Filled (EBAF, Level 3B) leverages off of the CERES Level 1-3 data products to produce a monthly TOA flux dataset that maintains the excellent radiometric stability of the CERES instruments while at the same time incorporating diurnal information from geostationary satellites in such a way as to minimize the impact of any geostationary imager artifacts that can occur over some geostationary domains and time periods. In order to ensure EBAF TOA fluxes satisfy known global mean energy budget constraints (e.g., based upon in-situ data from the Argo network, Roemmich et al. 2009), SW and LW TOA fluxes are adjusted within their range of uncertainty using an objective constrainment method (Loeb et al. 2009). Importantly, this is a one-time adjustment applied to the entire record. Therefore, the time-dependence of EBAF TOA fluxes is tied as closely as possible to the CERES instrument radiometric stability. Unlike other CERES data products, EBAF provides monthly regional clear-sky TOA fluxes that are free of missing regions by making optimal use of coincident CERES and MODIS measurements.

2.1 CERES Level 3 Flux Product Table

Table 2-2. A summary of the flux definitions, algorithms, and daily averaging criteria for the CERES Ed4A FluxByCldTyp, SSF1deg, SYN1deg, and EBAF products.

Flux criteria	FluxByCldTyp	SSF1deg	SYN1deg	EBAF
Satellites	Terra+Aqua	Single satellite	Terra+Aqua+GEO	Terra+Aqua+GEO
Calibration#	CERES instrument	CERES instrument	CERES instrument	Net balanced
Clear-sky source†	Sub-footprint	Footprint	Footprint (no GEO)	Sub-footprint & total region
SW flux observations§	SZA<82°	SZA<86.5°	SZA<86.5°	SZA<86.5°
SW Temporal Interpolation‡	none	Constant meteorology diurnal models	CERES+GEO-derived BB fluxes	CERES with empirical diurnal models
SW Twilight Flux*	no	no	no	yes
LW flux observations	SZA<82°, no nighttime	24-Hour observations	24-Hour observations	24-Hour observations
LW Temporal Interpolation^	none	Ocean/snow: linear interpolation Land: half-sine fit	CERES+GEO-derived LW fluxes	CERES+GEO-derived LW fluxes (net balanced)

The **CERES instrument** onboard calibration systems provide excellent stability over time. However, the CERES instrument calibration is not net balanced. The SSF1deg Ed4A 2003-2015 13-year mean Terra and Aqua net flux is 4.35 W m^{-2} and 4.97 W m^{-2}, respectively. The EBAF TOA fluxes are **net balanced** to satisfy known global mean energy budget constraints (e.g., based upon in-situ data from the Argo network, Roemmich et al. 2009). SW and LW TOA fluxes are adjusted within their range of uncertainty using an objective constrainment method (Loeb et al. 2009). Importantly, this is a one-time adjustment applied to the entire record.

† The CERES clear-sky observations are obtained from **CERES footprints** that have a cloud fraction less than 0.1% for the SSF1deg and SYN1deg products. Note the SYN1deg product does not incorporate GEO-derived clear-sky fluxes and relies solely on the CERES observed clear-sky fluxes. The GEO-based cloud mask was inadequate to properly identify clear-sky conditions. The FluxByCldTyp and EBAF product clear-sky fluxes combine the clear-sky **sub-footprint** derived fluxes and the observed CERES clear-sky footprint fluxes. The clear-sky sub-footprint fluxes are empirically derived from MODIS multi-channel radiances that are converted using narrowband to broadband coefficients based on homogeneous CERES clear-sky footprints. The EBAF product also includes clear-sky flux estimates for the **total region (cloud-removed)**, which includes both the observed clear-sky and cloudy portions. These new clear-sky fluxes are defined in a manner that is more in line with how clear-sky fluxes are represented in climate models. It is the monthly

regional Fu-Liou TOA computed flux difference from all regional CERES observations and the clear-sky fraction-weighted computed flux observations added to the EBAF observed clear-sky flux (Loeb et al. 2020).

§ CERES SW observed radiances are converted to fluxes using angular directional models (ADMs) for solar zenith angles (SZA) <86.5° (Su et al. 2015a). The CERES daytime cloud properties are retrieved for observations having a SZA<82° (Minnis et al. 2021). The FlxuByCldTyp product does not provide zonal or global flux means. For the SSF1deg, SYN1deg, and EBAF products, the monthly zonal SW flux for zones where the solar incoming flux is greater than zero is based on the last valid zonal albedo. The remaining nighttime zones with solar incoming fluxes of zero will have zonal SW fluxes of zero. The global flux is then the area weighted SW flux of all 1° zones. For the EBAF product, the SW twilight flux is also included in the computation of the zonal and global fluxes.

‡ CERES SW Temporal Interpolation converts SW flux observations into regional daily flux means by employing **constant meteorology diurnal models** (CERES SSF1deg stream) and assumes that the cloud properties at the time of the CERES observation remain constant, only accounting for changes in albedo with solar zenith angle (Doelling et al. 2013). The **CERES+GEO-derived broadband SW fluxes** enhance the CERES data by explicitly accounting for changes in clouds and radiation between CERES observation times by using 1-hourly imager data from five GEO satellites that cover 60°S-60°N at any given time (Doelling et al. 2013). **CERES with empirical diurnal models** (CERES SYN1deg stream) maintains the excellent CERES instrument calibration stability of SSF1deg while at the same time preserving the diurnal information found in SYN1deg. The regional empirical SW diurnal correction ratios are tied to the calendar month, surface type, latitude, and GEO diurnal asymmetry ratio. The GEO diurnal asymmetry ratio quantifies the GEO morning and afternoon SW flux difference without introducing GEO artifacts (Loeb and Doelling 2020).

***** The **SW twilight flux** contribution is the diffraction of sunlight in the atmosphere that accounts for reflected SW fluxes for time periods during the day where the solar zenith angle is greater than 90°. This twilight flux is added to the daily/monthly averaged flux (Kato, S., and N. G. Loeb, 2003).

^ CERES converts LW flux observations into regional daily flux means by **linear interpolation** between CERES LW observations over ocean and snow surfaces and by employing a **daytime half-sine fit** symmetric about local noon (peak heating) model to account for daytime land heating. The **CERES+GEO-derived broadband fluxes** enhance the CERES data by explicitly accounting for changes in clouds and radiation between CERES observation times using 1-hourly imager data from five GEO satellites that cover 60°S-60°N at any given time (Doelling et al. 2013). The GEO LW narrowband to broadband algorithm employs both the GEO IR window (~11μm) and water vapor (~6.5μm) channels, which have first been inter-calibrated with Aqua-MODIS. The GEO LW algorithm uses empirical coefficients based on Aqua SSF footprint data. The GEO-derived LW fluxes are normalized to CERES fluxes regionally to ensure that the daily/monthly fluxes are tied to the CERES calibration. The **EBAF** product uses the SYN1deg LW fluxes after they have been net balanced.

3.0 Cautions and Helpful Hints

The CERES Science Team notes several CAUTIONS and HELPFUL HINTS regarding the use of CERES_FluxByCldTyp-Day/Month Ed4A:

- The CERES_FluxByCldTyp-Day/Month_Ed4A products can be visualized, subsetted, and ordered from: https://ceres.larc.nasa.gov/data/.
- This is the initial release of the CERES_FluxByCldTyp-Day/Month_Ed4A product. Users are encouraged to provide the CERES science team any suggestions to improve or to increase the usability of this product by emailing LaRC-CERES-Help@mail.nasa.gov.
- A full list of parameters on the CERES_FluxByCldTyp-Day/Month_Ed4A products is contained in their respective Data Product Catalogs (PDF):
  FluxByCldTyp-Day Data Product Catalog
  FluxByCldTyp-Month Data Product Catalog
- Users should be aware that some of the key inputs used to produce the CERES products change at various times during the data record. Such changes, if large enough, may introduce spurious, unphysical jumps in the record. In the past, these changes were reflected in each CERES data product's version through a letter change (e.g., SRBAVG Edition2A, Edition2B, etc.). However, this proved cumbersome and confusing to many users. Therefore, for the FluxByCldTyp product, letter changes will only reflect a reprocessing of the data record (e.g., due to a code bug). Major algorithm improvements will be noted as Editions. Changes to inputs are documented at the following web site: https://ceres.larc.nasa.gov/data/general-product-info/#ceres-input-data-sources. The web site provides a timeline of all input data source changes to date used to produce the FluxByCldTyp Ed4A products. Users are advised to use this information as a reference in their analysis of FluxByCldTyp products.
- The Aqua satellite experienced an anomaly preventing any data transmittal from August 16 to September 3, 2020. CERES processing filled this Aqua gap with the SSF NOAA-20 Ed1B fluxes and clouds from August 16-31. September 1-3 was not filled.
- The CERES FluxByCldTyp-Day/Month Ed4A are based on both the Terra and Aqua SSF Ed4A footprint products. There are two CERES instruments on the Terra and Aqua satellites. Only the CERES instrument that is in cross-track mode is used, since it provides uniform spatial distribution of footprints. No Rotating Azimuth Plane Scan (RAPS) mode is used. All CERES Terra/Aqua instruments are calibrated to be on the same radiometric scale beginning with CERES Edition 3. For Terra, the FM1 instrument spends the most time in crosstrack mode. For Aqua, FM4 was the prime crosstrack instrument prior to March 2005, when the SW channel failed. After March 2005, Aqua FM3 was permanently placed in crosstrack mode. The CERES input data sources page (https://ceres.larc.nasa.gov/data/general-product-info/#ceres-instruments-in-crosstrack-scan-mode) shows the Terra and Aqua instrument that is in cross-track mode.
- Processing is performed on a nested grid (see Table 3-1). This grid uses 1° equal-angle regions between 45°N and 45°S and maintains area consistency at higher latitudes. The final products contain a complete 360x180 1° grid created by replication.

Table 3-1. CERES nested grid.

Latitude segment	# of zones in segment	Longitude extent (°)	# of regions/zone	# of regions in segment
Equator to 45°	90	1°	360	32400
45° to 70°	50	2°	180	9000
70° to 80°	20	4°	90	1800
80° to 89°	18	8°	45	810
89° to 90°	2	360°	1	2
Total	180	-	-	44012

Fluxes

- The FluxByCldTyp Ed4A product only incorporates daytime CERES observed SW and LW fluxes with a solar zenith angle less than 82°. The MODIS daytime cloud optical depth retrievals are based on visible channels, which allow for a greater range of optical depths than those based strictly on IR channels. To avoid inconsistent cloud-type classification between daytime and nighttime cloud retrievals, the FluxByCldTyp is limited to daytime observations. The FluxByCldTyp dataset includes both Terra and Aqua instantaneous gridded input. If both Terra and Aqua measurements are coincident, the measurement with the lowest view zenith angle is retained.
- For Edition 4, the SW twilight flux is only added in the EBAF product, since the EBAF product is a net flux balanced product. The twilight flux contribution is from the diffraction of sunlight in the atmosphere that accounts for reflected SW fluxes for time periods during the day where the solar zenith angle is greater than 90°. This twilight flux is added to the daily/monthly averaged flux (Kato, S., and N. G. Loeb, 2003). The twilight flux value is much smaller than the CERES instrument calibration adjustment. The FluxByCldTyp Ed4A product does not include the twilight flux.
- The FluxByCldTyp Ed4A product is anchored to the CERES instrument calibration and is not energy balanced. The CERES FluxByCldTyp, SSF1deg, and SYN1deg level 3 products are all tied to the CERES instrument calibration. Despite recent improvements in satellite instrument calibration and the algorithms used to determine SW and LW outgoing TOA radiative fluxes, a sizeable imbalance persists in the average global net radiation at the TOA from CERES satellite observations. With the most recent CERES Edition4 instrument calibration improvements, the SSF1deg Edition4A net imbalance is ~+5 W m^{-2}, which is much larger than the expected observed ocean heating rate of ~0.71 W m^{-2} (Johnson et al. 2016). If net balanced fluxes are required for the evaluation of climate models, for example, we recommend using the CERES EBAF Ed4A product. The EBAF dataset uses an objective constrainment algorithm to adjust SW and LW TOA fluxes within their ranges of uncertainty to remove the inconsistency between average global net TOA flux and heat storage in the Earth-atmosphere system.

- The CERES Edition 4 solar irradiance is from SORCE that is updated daily (SORCE Level 3 Total Solar Irradiance Version 15 available from: http://lasp.colorado.edu/sorce/data/tsi_data.htm. The SORCE total solar irradiance is ~1361 W m^{-2}. The SORCE observed solar irradiance will vary over the 11-year sunspot cycle with an amplitude of ~0.1%.
- A processing glitch was discovered in the daily TSI file. The TSI daily fluxes during August 2019 and May through November 2020 (shown as the red values in Figure 3-1) were found to be scaled incorrectly resulting in a daily flux that was biased by ~ +0.8 W m^{-2}. The incorrect daily TSI fluxes (based on TSIS-1 TIM Version 3) were correctly scaled to the SORCE Version 15 reference and updated during February 2021. The FluxByCldTyp product was impacted during August 2019 and May 2020 through July 2020. The resultant global averaged daily and monthly fluxes were found to be ~0.2 W m^{-2} too large out of a 20-year mean TSI flux of 339.88 W m^{-2}.

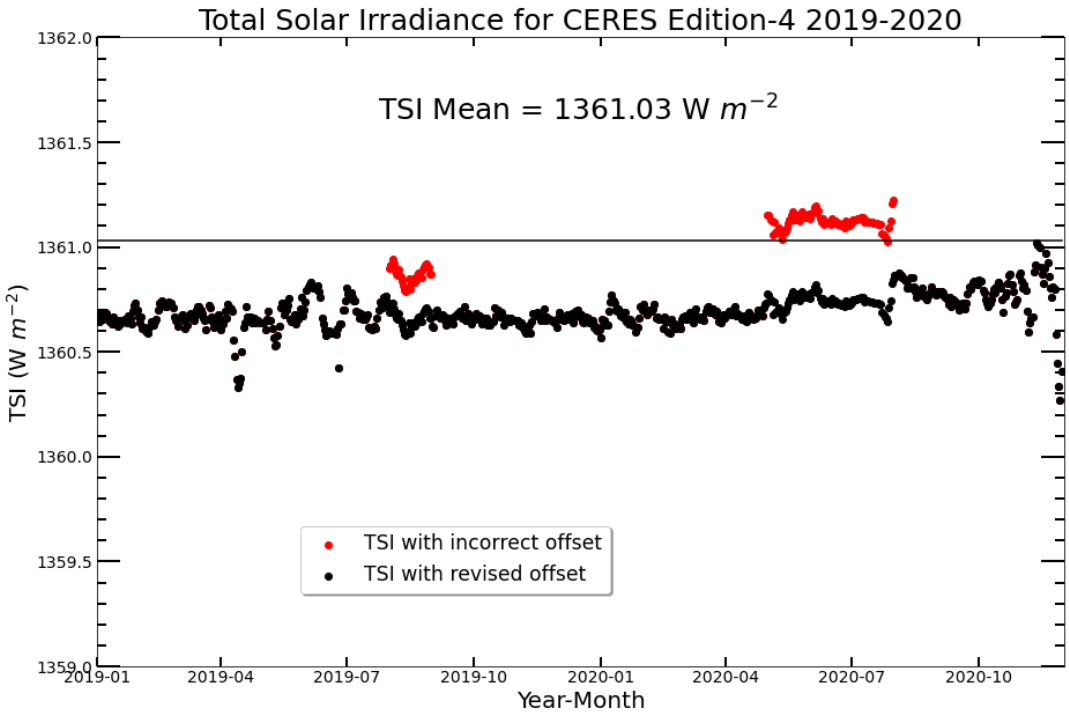

Figure 3-1. TSIS-1 TIM Version 3 at 1 AU incorrect scaling (red daily values) compared to the correct scaling (black daily values).

- Performing monthly deseasonalization or annual anomalies based on the 365-day calendar year (as opposed to 365.256 days for Earth to orbit the sun) may introduce unwanted variability in the CERES fluxes. Care must be taken when interpreting monthly anomalies. Please see the SSF1deg_Ed4A_Data_Quality_Summary_Appendix (section 10) for more information and examples.
- The FluxByCldTyp Ed4A clear-sky fluxes are virtually spatially complete for regions with daytime measurements within a solar zenith angle of 82°. Both the FluxByCldTyp and EBAF product clear-sky fluxes are the combination of clear-sky footprint and sub-footprint derived

fluxes. However, the EBAF monthly product ensures all regions have an associated clear-sky flux by using climatology if no sub-footprint observations are available (Figure 3-2, left panel). The SSF1deg-Day/Month product relies on completely clear-sky (cloud fraction <0.1%) 20-km nominal footprints. Over very cloudy regions, clear-sky spatial data gaps occur in the SSF1deg product if no clear-sky footprints are observed (Figure 3-2, right panel). Although the FluxByCldTyp relies on sub-footprint clear-sky fluxes, the polar regions do not have an associated SW flux, since the product limits the observed CERES observations within 82° in solar zenith angle.

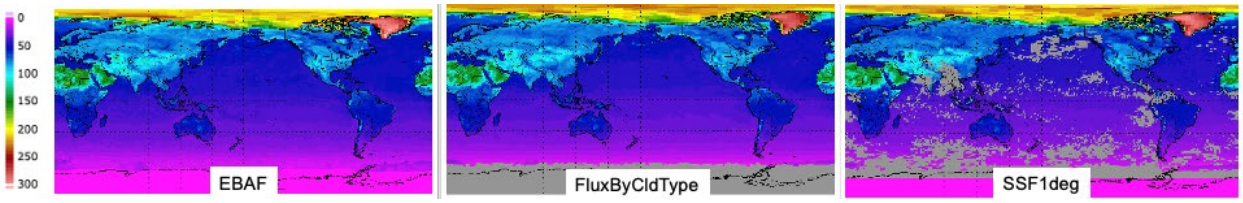

Figure 3-2. The July 2002 EBAF, FluxByCldTyp-Month, and SSF1deg-Month Terra+Aqua SW clear-sky fluxes. The SW units are in W m^{-2}. These plots illustrate the clear-sky spatial coverage of the individual products.

- The FluxByCldTyp daily fluxes are defined in GMT. This facilitates comparisons with climate models. For regions near Greenwich, the local and GMT days are similar. However, for regions near the west side of the dateline (170°E) the afternoon of the previous local day and the morning of the following local day are combined with local midnight occurring during the middle of the GMT day. The SSF1deg and SYN1deg products are also GMT-based.
- Zonal and global parameters means are not computed for the FluxByCldTyp Ed4A product. The geographical distribution of the spatial gaps due to insufficient sampling will not provide a true representation of the zonal and global flux and cloud means. Fluctuations in the daily global mean are more likely to be attributed to spatial sampling and do not reflect the natural variation.
- There are occasional data gaps in the CERES observations. The most noticeable data gaps are listed in Table 3-2. Also, small data gaps occur over the equator where the Terra and Aqua CERES orbit swaths are not contiguous.

Table 3-2. Dates of the major data gaps in the Terra and Aqua CERES records.

Terra	Aqua
April 26-27, 2000	July 1-3, July 30-Aug 6, 2002
August 6-18, 2000	October 1-14, 2004 (instrument anomaly)
June 15-July 2, 2001	March 30-31, 2005
March 20-28, 2002	
December 17-24, 2003	
February 19-27, 2016	

- The Terra and Aqua CERES instruments are placed on a common radiometric scale at the start of mission (March 2000 for Terra; July 2002 for Aqua). For a detailed description of the

radiometric scaling, please see the following link (slides 20-70): http://ceres.larc.nasa.gov/documents/STM/2010-04/2_Priestley_0410_STM_Newport News.pdf. The CERES SSF1deg-NPP Ed1 was not radiometrically scaled to either Terra or Aqua. The user is advised that there may be flux differences due to calibration differences when comparing NPP with either Terra or Aqua. The CERES SSF1deg NPP Ed2 as well as the SSF1deg NOAA20 Ed 2 product will be radiometrically scaled with Terra and Aqua.

- A bug was fixed in the calculation of daily albedo, and the corrected data was made available on the CERES Ordering Tool on February 3, 2022. In addition, daily albedo is now constrained to be 1 in rare instances where the reflected SW flux exceeded the incoming solar flux. Consequently, the monthly mean SW flux and albedo may be slightly different than it was originally, due to this albedo constraint.
- See section 2.1 for a summary of the CERES Ed4A FluxByCldTyp, SSF1deg, SYN1deg, EBAF product flux definitions.

Clouds

- The FluxByCldTyp cloud fraction is based on MODIS pixels having an associated cloud effective pressure and optical depth retrieval. The FluxByCldTyp cloud fraction does not include the non-retrieved pixels as is the case in the SSF1deg and EBAF products. The CERES cloud property algorithm was designed to minimize the number of non-retrieved cloud pixels. The CERES footprint angular directional models are selected by scene type defined by cloud fraction, optical depth and phase. If a CERES footprint has an insufficient number of cloud-retrieved pixels, the CERES radiance is converted to flux using a neural network algorithm. The FluxByCldTyp product does not include footprints with neural network associated fluxes.
- The FluxByCldTyp Ed4A product is based on the Terra SSF Ed4.1 product, which is an improvement over the SSF1deg Ed4.0 product. During February 2016, the Terra satellite underwent a spacecraft anomaly, which resulted in a two-week outage. The Terra-MODIS 6.7-µm and 8.6-µm channels suffered from induced cross talk detector-to-detector striping. MODIS Collection 6.1 mitigated the Terra-MODIS 6.7-µm and 8.6-µm channel detector-to-detector striping. The Terra-MODIS cloud properties were rerun from February 2016 until March 2018 using MODIS collection 6.1. The Aqua-MODIS cloud properties were also rerun between February 2016 and March 2108 using Collection 6.1 for consistency. See pages 3 and 4 in the following presentation https://ceres.larc.nasa.gov/documents/STM/2019-05/08_CERES_STM_TISA_2019_05_final.pdf.
- The MODIS Collection 6.1 visible channel radiances were radiometrically scaled to Collection 5.0 in order to retrieve consistent cloud properties throughout the CERES record beginning in 2000. Collection 5 was run from the beginning of the Terra and Aqua records until February 2016; after that point Collection 6.1 was utilized and is still used in forward processing.
- The FluxByCldTyp Ed4A product optical depth is based on the 3.7-µm channel, except over snow where it is based on the 1.2-µm channel.
- The FluxByCldTyp Ed4A product cloud properties are based on the MODIS Ed4A cloud algorithm (Trepte et al. 2019, Minnis et al. 2021, Yost et al. 2021) and are contained in the CERES SSF Ed4A product. The quality of the MODIS cloud properties used in CERES are

summarized in the SSF Ed4A Data Quality Summary.

- The CERES FluxByCldTyp Ed4A product is not based on the NASA Goddard MODIS cloud properties. The Goddard cloud properties, excluding cloud amount, are determined from pixels with confident retrievals. Figure 3-3 (left panel) shows the FluxByCldTyp and MOD08 cloud fraction from the mask. The global mean cloud fraction difference is within 2.4%. The comparison of the FluxByCldTyp Ed4A and the Goddard MOD08 product *retrieved* cloud fractions (pixel must have an associated optical depth and cloud effective pressure) is shown in Figure 3-3 (right panel). The global amount difference is 19.7%. We advise using the CERES MODIS or FluxByCldTyp cloud properties when evaluating the cloud-type fluxes.

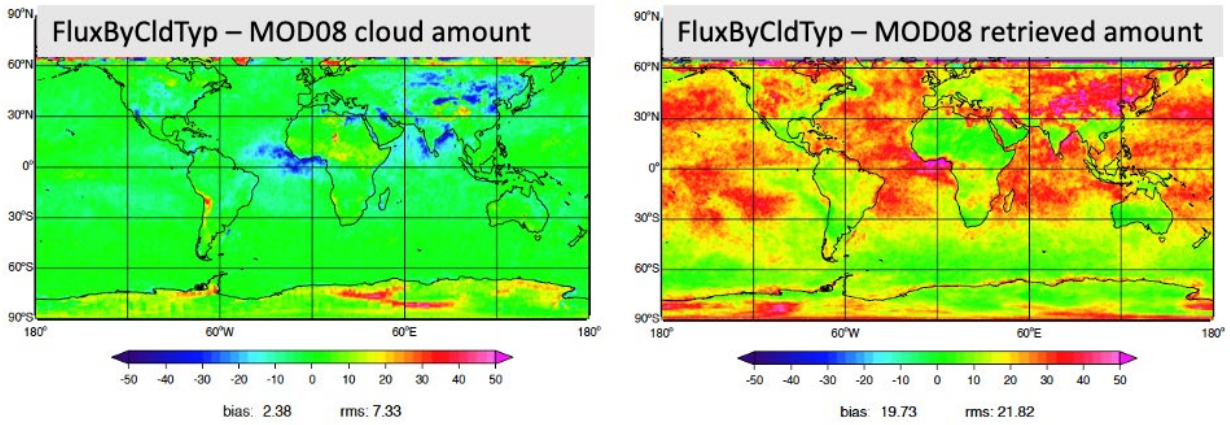

Figure 3-3. The January 2010 CERES FluxByCldTyp (Terra-only) minus Goddard MOD08-Terra **cloud** amount (left panel) and minus the Goddard MOD08-Terra **retrieved** amount (right panel) (must have an associated cloud optical depth and cloud effective pressure). The global means and 1° regional RMS error are shown at the bottom of the plots.

Auxiliary Parameters

- The FluxByCldTyp product frequency statistics allow the user to determine sufficient cloud-type sampling required for a robust flux measurement. The lack of cloud-type sampling is usually manifested by noisy regional or temporal flux values. The FluxByCldTyp-Day/Month products provide the total number of regional SW and LW cloudy and clear-sky flux measurements observed over the day or month, respectively. The monthly product also includes the number of days with measurements.

4.0 Version History

This is the initial release of the CERES FluxByCldTyp product. If any issues are found or if the algorithms are updated a new version will be released and the version history will be updated here. Users are encouraged to provide the CERES science team any suggestions via LaRC-CERES-Help@mail.nasa.gov to improve or to increase the useability of this product.

5.0 Accuracy and Validation

5.1 FluxByCldTyp Ed4A Uncertainties

The monthly 1°x1° regional all-sky SW flux uncertainty is due to: 1) CERES instrument calibration uncertainty of 1 W m^{-2} (1σ), 2) the radiance-to-flux conversion error of 1 W m^{-2} (1σ) (Su et al. 2015b), and 3) the all-sky diurnal correction (based on constant meteorology) uncertainty of 6 W m^{-2} (Doelling et al. 2013). The diurnal correction uncertainty value is based on comparisons with Geostationary Earth Radiation Budget (GERB) observed broadband SW fluxes. The diurnal correction may be overestimated, since the GERB geostationary domain has a disproportionate number of strong diurnal cycle regions as compared with the globe. The combined monthly regional all-sky SW flux uncertainty is 6.2 W m^{-2}. The daily regional all-sky SW diurnal uncertainty is 20 W m^{-2} (Doelling et al. 2013). These uncertainties are for all-sky fluxes, the 42 cloud-type and clear-sky SW fluxes would have greater uncertainties.

The monthly 1°x1° regional all-sky LW flux uncertainty is due to: 1) CERES instrument calibration of 1.8 W m^{-2} (1σ), 2) the radiance to flux conversion 0.75 W m^{-2} (1σ) (Su et al. 2015b), and 3) the diurnal correction of 6 W m^{-2} (Doelling et al. 2016). Since FluxByCldTyp does not include any nighttime measurements the diurnally averaged LW flux is not available. The FluxByCldTyp LW flux is an average of the daytime measurements and does not represent a true 24-hour mean.

The cloud property uncertainties may be obtained from the SSF Ed4A Data Quality Summary: https://asdc.larc.nasa.gov/documents/ceres/quality_summaries/CER_SSF_Terra-Aqua_Edition4A.pdf.

5.2 FluxByCldTyp Ed4A and SSF Ed4A Instantaneous Footprint Flux Comparisons

This section validates the FluxByCldTyp sub-footprint narrowband to broadband derived fluxes before they are normalized to the observed CERES footprint flux. The MODIS 5-channel narrowband to broadband model multi-linear regression coefficients are computed from uniform scene type SSF footprint MODIS channel radiances and the CERES flux. The SW narrowband to broadband look up table (LUT) has 9 solar zenith angle, 7 view angle and 9 relative azimuth angle bins and is also based on 7 surface types and whether the footprint is overcast or clear. The 7 surface classifications are ocean, forests, savanna, grassland/cropland, dark desert, bright desert and snow/ice. The LUT is not based on any cloud properties and strictly relies on five channels of MODIS imager radiances. The LW narrowband to broadband LUT has 7 view angle and 4 precipitable water bins, 7 surface types, and clear/overcast bins. The narrowband to broadband monthly LUTs were produced from Terra and Aqua SSF Ed4A 2007 to 2011 data.

Figure 5-1 shows the first 10 days of January 2010 narrowband to broadband computed sub-footprint fluxes averaged into a footprint flux and then compared with the observed CERES footprint flux. Of the 9.2 million total footprints, 6.1 million were non-homogeneous and had more than two or more scene types. The narrowband to broadband footprint SW and LW flux had a bias of -0.6% and -0.1%, respectively. The computed and observed SW and LW flux standard deviation was 6.0% and 2.6%, respectively.

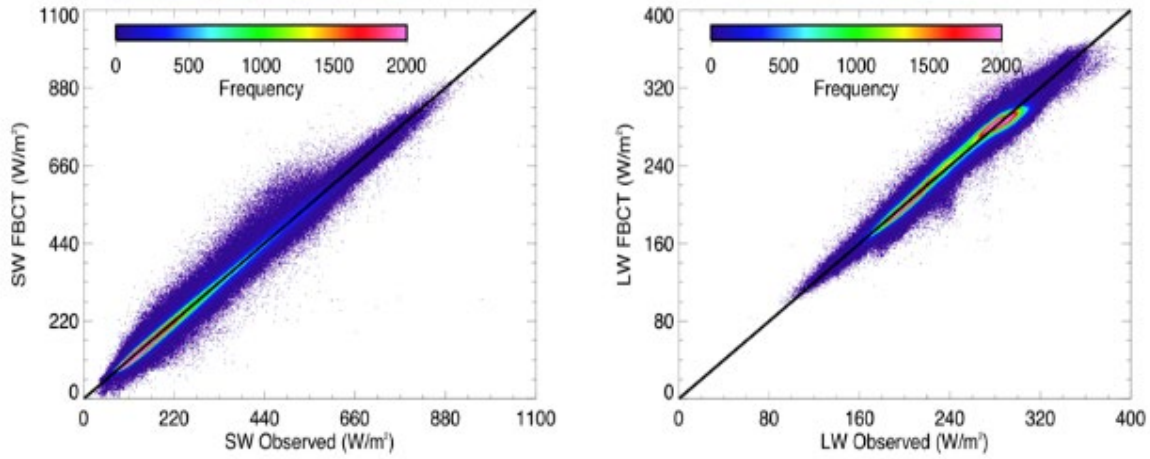

Figure 5-1. The FluxByCldTyp narrowband to broadband computed and observed (left panel) SW and (right panel) LW non-homogeneous Terra and Aqua footprint flux frequency plot during January 1-10, 2010. The observed SW and LW mean fluxes are 236.17 W m^{-2} and 241.64 W m^{-2}, with a bias of -1.43 W m^{-2}, and -0.27 W m^{-2} and associated standard deviation of 14.27 W m^{-2} and 6.19 W m^{-2}, respectively.

More importantly, the FluxByCldTyp narrowband to broadband derived fluxes should not be biased according to cloud fraction, cloud effective pressure, optical depth, precipitable water, surface type, solar zenith angle, and view zenith angle. The FluxByCldTyp narrowband to broadband derived minus CERES flux difference is plotted as a function of the cloud properties, surface type, solar and viewing geometry, and precipitable water in Figure 5-2 and Figure 5-3. There are no observable dependencies in the FluxByCldTyp narrowband to broadband derived fluxes.

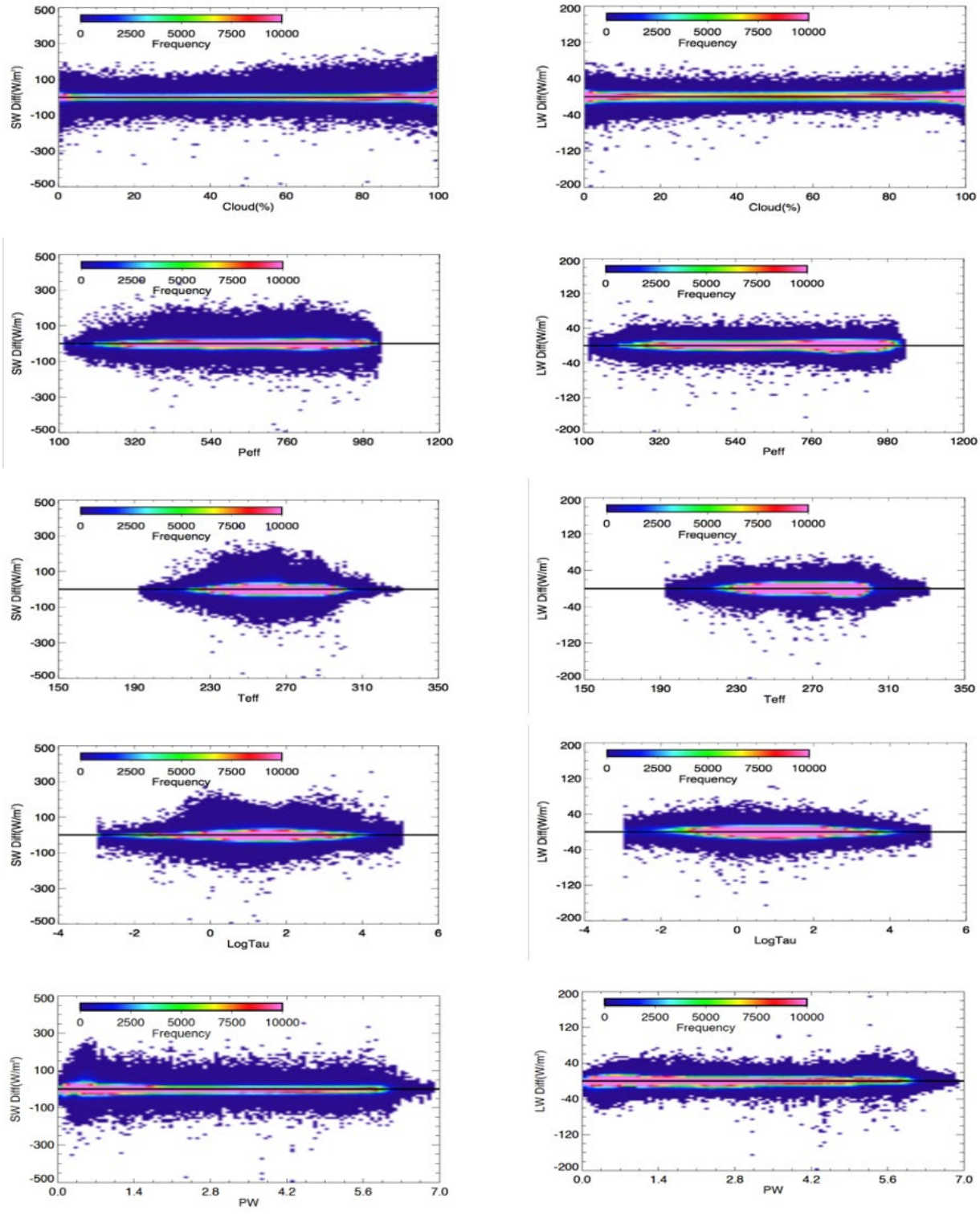

Figure 5-2. The FluxByCldTyp narrowband to broadband computed minus observed (left panels) SW and (right panel) LW non-homogeneous Terra and Aqua footprint flux (W m^{-2}) frequency plots during January 1-10, 2010 as a function of cloud fraction (%), cloud effective pressure (Peff in mb), cloud effective temperature (Teff in K), logarithm of cloud optical depth (LogTau), and precipitable water (PW in cm).

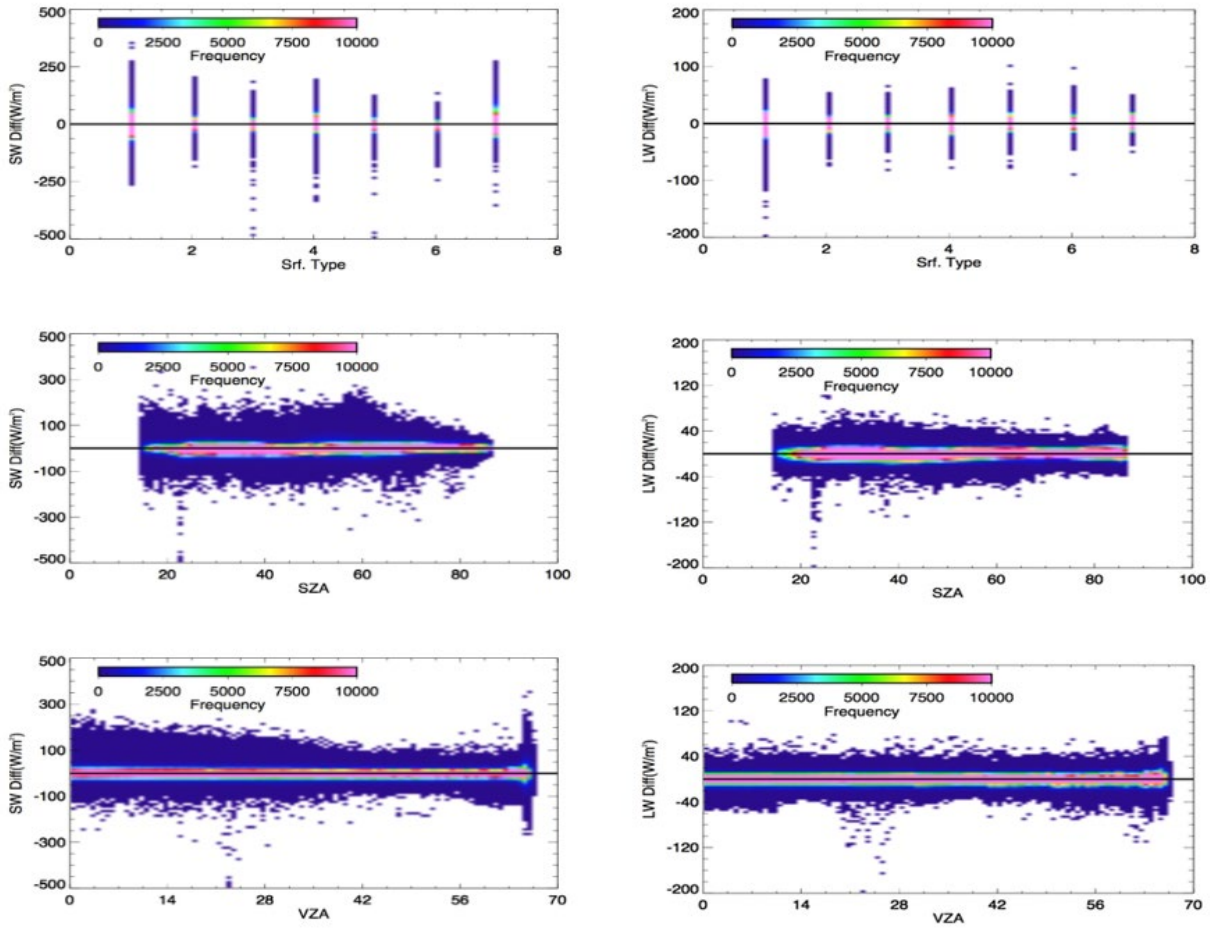

Figure 5-3. The FluxByCldTyp narrowband to broadband computed minus observed (left panels) SW and (right panel) LW non-homogeneous Terra and Aqua footprint flux (W m^{-2}) frequency plots during January 1-10, 2010 as a function of surface type (1=ocean, 2=forest, 3=savanna, 4=grass/croplands, 5=dark deserts, 6=bright deserts, 7=snow/ice), solar zenith angle (SZA in degrees) and view zenith angle in degrees.

5.3 FluxByCldTyp Ed4A and SSF1deg Ed4A Jan 2010 Regional Comparisons

The combined regional FluxByCldTyp cloud-type and clear-sky fluxes should equal the SSF1deg Terra+Aqua all-sky flux, if the sub-footprint fluxes were properly derived. The individual FluxByCldTyp cloud-type fluxes and clear-sky fluxes are weighted by their respective cloud-type fractions into an all-sky flux. The FluxByCldTyp (Terra-only) all-sky and clear-sky fluxes are compared to the SSF1deg-Month-Terra fluxes and displayed in Figure 5-4. This comparison will highlight both the consistencies and differences between the FluxByCldTyp and SSF1deg products. Refer to Section 2.1 for a discussion of the SW and LW flux differences between the CERES product L3 products. The SSF1deg Terra+Aqua dataset is not available to the public but employs the same code as the single satellite SSF1deg product.

Figure 5-4 (upper right panel) shows that the all-sky SW fluxes are similar between the FluxByCldTyp and SSF1deg products. Clearly, both products do not consider nighttime SW measurements (solar zenith angle >86.5°). However, the FluxByCldTyp does not include SW measurements between a solar zenith angle of 82° and 86.5°. There are two zones where the observed average solar zenith angle differs between FluxByCldTyp and SSF1deg and are shown in the bottom right panel in Figure 5-5. The zone between 68° and 78° South clearly impacts the all-sky SW flux difference. The regional noise near the dateline in the Pacific Ocean usually indicates an hourly overpass at the beginning or end of the month that exists in one dataset but not the other. Remarkably, whether the SW fluxes are temporally interpolated (SSF1deg) or the average of the equivalent daily fluxes are averaged (FluxByCldTyp), the SW monthly mean flux is very similar. This is because the regional Terra and Aqua overpass are symmetric about noon, allowing simple averaging of the daily equivalent fluxes.

Figure 5-4 (upper left panel) displays the clear-sky SW flux difference between the FluxByCldTyp and SSF1deg products. The very cloudy non-polar regions show a larger FluxByCldTyp clear-sky SW flux. The FluxByCldTyp product includes sub-footprint fluxes, which have a smaller spatial domain than the 20-km nominal CERES footprint used exclusively in the SSF1deg product. The smaller non-polar sub-footprints are located in more cloudy regions and tend to contain more aerosols. The Antarctic zone of greater SSF1deg clear-sky SW flux coincides with the zone with observations having a solar zenith angle between 82° and 86.5°. It is unclear why there is zone of larger land SSF1deg clear-sky SW fluxes at ~45°N.

Figure 5-4 (lower right panel) presents the all-sky LW flux difference between FluxByCldTyp and SSF1deg products. Land regions distinctly show a larger FluxByCldTyp all-sky LW flux, since the product does not include nighttime observations, whereas the SSF1deg incorporates both daytime and nighttime measurements. The FluxByCldTyp product does not provide a valid 24-hour all-sky LW flux. Over ocean regions the regional daytime FluxByCldTyp LW flux monthly mean flux is similar to the SSF1deg all-sky LW monthly mean flux, since ocean surface temperatures are nearly the same for daytime and nighttime conditions. The noisy all-sky LW flux regional differences are due to variations in the day and night cloud height and thickness fluctuations.

Figure 5-4 (lower left panel) depicts the FluxByCldTyp and SSF1deg product clear-sky LW fluxes. The difference is very similar to the all-sky LW difference except over ocean regions. The FluxByCldTyp also includes the smaller sub-footprint fluxes that are located near cloud edges and typically are more humid than the larger 20-km nominal CERES clear-sky footprints. The atmospheric humidity tends to decrease the TOA clear-sky flux. This is especially the case for areas with high clouds.

The combined regional FluxByCldTyp cloud-type cloud properties should equal the SSF1deg daytime cloud properties. For this comparison, shown in Figure 5-5, the FluxByCldTyp product was run with only Terra observations in order to match the SSF1deg-Terra daytime cloud properties. Note the excellent agreement except for locations where measurements having solar zenith angles between 82° and 86.5 are observed (See Figure 5-5, bottom right panel). The noisy FluxByCldTyp and SSF1deg cloud amount differences are within 3%.

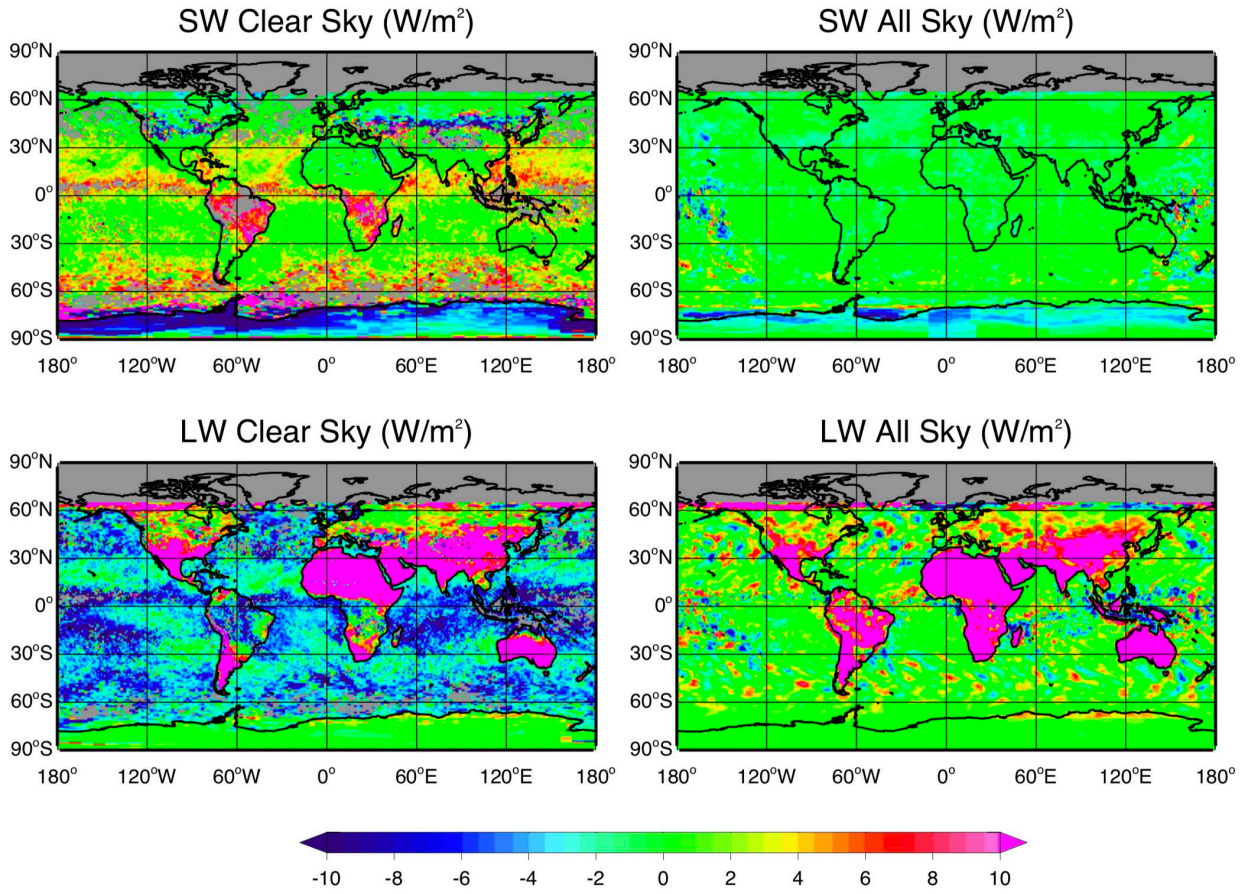

Figure 5-4. The January 2010 FluxByCldTyp-Month all-sky SW minus SSF1deg-Month-Terra+Aqua clear-sky SW, all-sky SW, clear-sky LW, and all-sky LW.

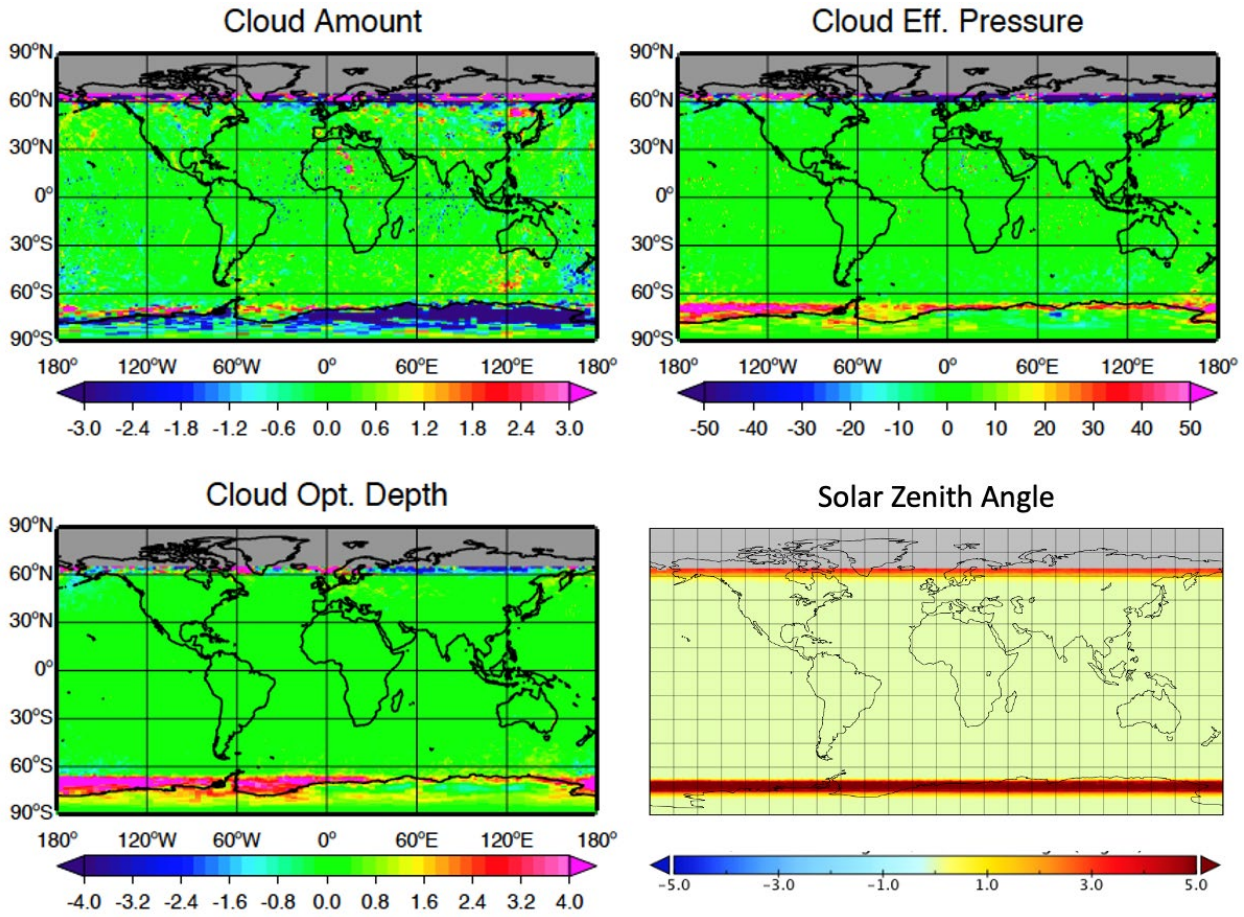

Figure 5-5. The January 2010 FluxByCldTyp-Month (Terra-only) minus SSF1deg-Month-Terra daytime cloud amount (%), cloud effective pressure (mb), cloud optical depth (unitless), and solar zenith angle (deg).

5.4 FluxByCldTyp Ed4A, and SSF1deg Ed4A Global Mean Comparisons

In order to demonstrate that the FluxByCldTyp individual cloud-type fluxes and clouds are of climate quality and are robust enough to determine long-term trending, the July 2002 to December 2018 FluxByCldTyp global mean flux and cloud anomalies are compared with the SSF1deg product anomalies. The combined 42 cloud-type and clear-sky fluxes are fraction weighted to compute the total or all-sky regional flux. The FluxByCldTyp all-sky SW flux can then be compared to the SSF1deg Terra+Aqua all-sky SW flux. To compare FluxByCldTyp SW fluxes with SSF1deg and EBAF, only measurements with solar zenith angle less than 82° are used to compute the global means for all three products in Figure 5-6. This figure shows the excellent agreement of the global mean all-sky and clear-sky SW flux anomalies. It is advised when comparing regional FluxByCldTyp individual cloud-type flux trends to make sure that there is sufficient sampling. A noisy month-to-month flux would suggest insufficient sampling. If there are a few monthly outlier fluxes, they should probably not be included in a time series analysis. The sampling can be increased by combining multiple regions, multiple months, or cloud types.

Similarly, the FluxByCldTyp (Terra-only) and SSF1deg-Terra global cloud amount and cloud effective pressure means also show agreement in Figure 5-7. The slight difference in cloud optical depth is associated with different temporal averaging; the SSF1deg product uses temporal interpolation across the day, and the FluxByCldTyp product uses simple averaging of daytime measurements.

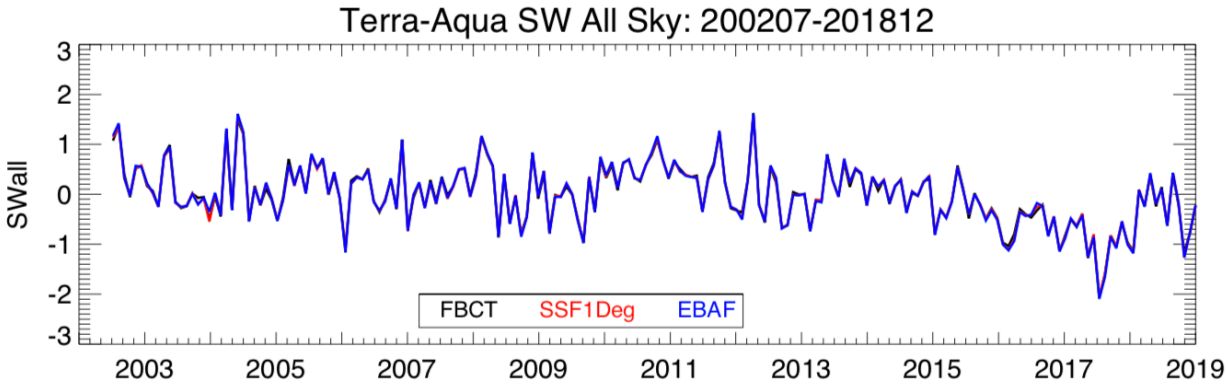
Terra-Aqua SW All Sky: 200207-201812
SWall
FBCT
SSF1Deg
EBAF

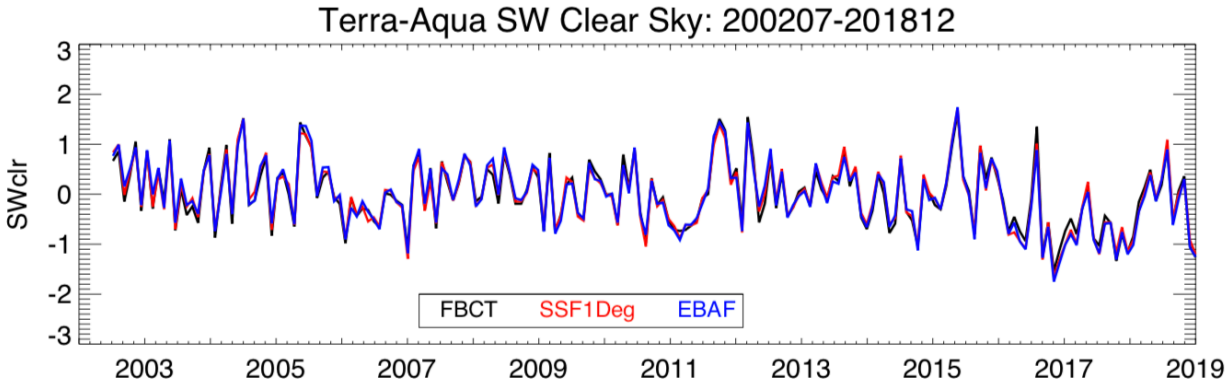
Terra-Aqua SW Clear Sky: 200207-201812
SWclr
FBCT
SSF1Deg
EBAF

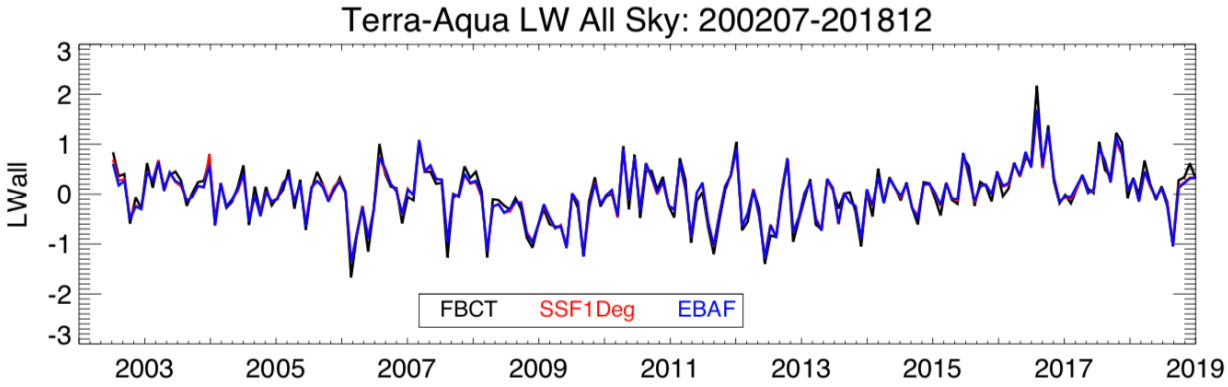
Terra-Aqua LW All Sky: 200207-201812
LWall
FBCT
SSF1Deg
EBAF

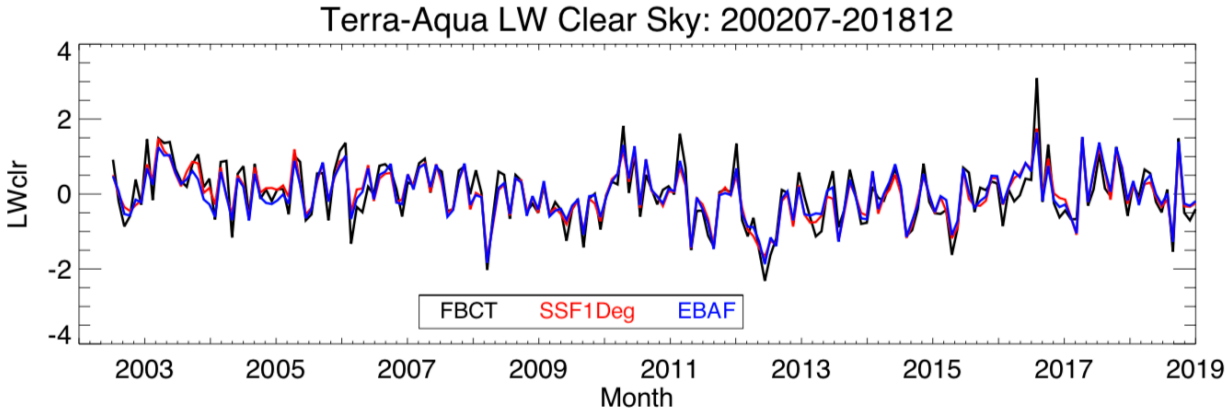
Terra-Aqua LW Clear Sky: 200207-201812
LWclr
FBCT
SSF1Deg
EBAF
Month

Figure 5-6. The FluxByCldTyp Ed4A, SSF1deg-Terra+Aqua Ed4A, and EBAF Ed4.1 all-sky SW (top panel), clear-sky SW (second panel), all-sky LW (third panel), and clear-sky LW (bottom panel) global mean flux anomalies (July 2002 to December 2018), computed from regions having observations with solar zenith angle <82°. In this figure, these are not true global means and thus differ from the SSF1deg and EBAF product global flux means.

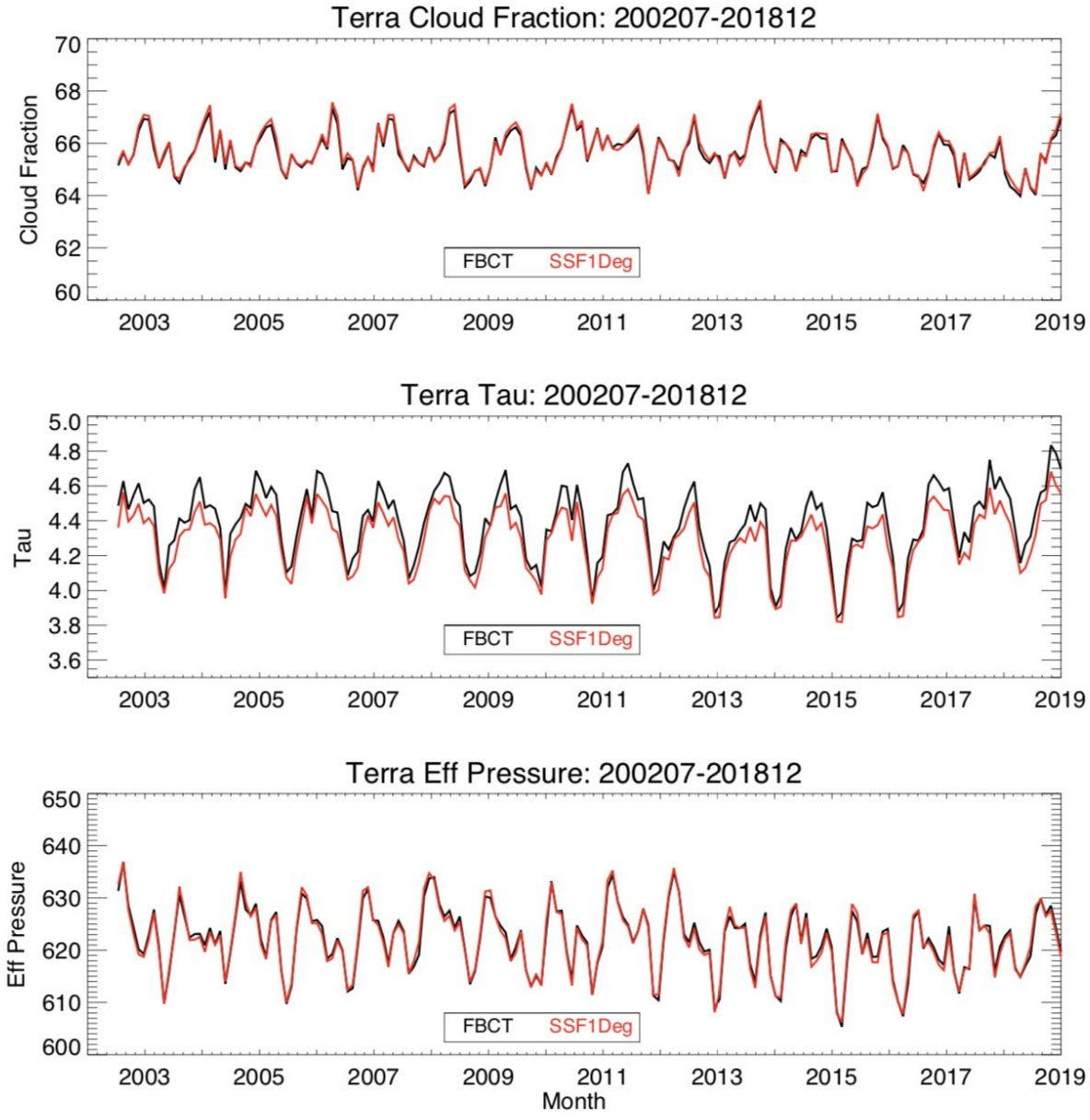

Figure 5-7. The FluxByCldTyp, SSF1deg-Terra daytime cloud amount in % (top panel), cloud optical depth (middle panel), and cloud effective pressure in mb (bottom panel) global mean anomalies (July 2002 to December 2018) computed from regions having observations with solar zenith angle <82°. This is not a true global mean.

5.5 FluxByCldTyp-Month Ed4A Radiative Kernel Comparison

The FluxByCldTyp product can easily produce radiative kernels, which are defined as the clear-sky flux minus the cloud-type (overcast) flux divided by 100, which is the overcast cloud amount in percentage. The radiative kernel provides the flux sensitivity as a function of cloud type given a 1% change in cloud-type amount. Figure 5-8 illustrates the global mean LW, SW and Net flux radiative flux kernels computed from FluxByCldTyp during 2010. The upper right corner of the cloud pressure/optical depth (Pc-Tau) matrix is representative of deep convective clouds. These clouds significantly reduce the outgoing LW flux (left panel in Figure 5-8) but also increase the SW reflected flux. However, it seems that the net flux indicates that the SW flux increase is slightly greater than the LW flux reduction. This suggests that if the deep convective cloud amount is increased by 1%, the global net flux would decrease by 0.8 W m^{-2}. As predicted, an increase in thick low clouds will cool the climate, whereas an increase in thin high clouds will warm the climate.

The 2010 global mean FluxByCldTyp radiative kernel agrees overall with Figure 1 of Zelinka et al. (2012). Note that the Zelinka et al. (2012) kernel splits the first optical depth (0 to 1.3) bin into two parts. The first part of the optical depth bin encompasses an optical depth between 0 and 0.3. It is very difficult to identify and retrieve cloud properties for these optically thin clouds. The CERES MODIS cloud algorithm can only effectively retrieve optical depths greater than 0.3. The thick (60 to 379) low (1000-800 mb) clouds are not well sampled and were mostly observed over the arctic with large solar zenith angle conditions. To achieve an optical depth greater than 60 for a cloud layer capped at 600 mb is not a common occurrence. Note that the CERES MODIS algorithm has an optical depth limit of 150. The CERES-based high resolution Pc-Tau bin radiative kernel could not have been computed without performing the MODIS narrowband to broadband algorithm by cloud type. The agreement with results from Zelinka et al. (2012) shows the algorithm works well.

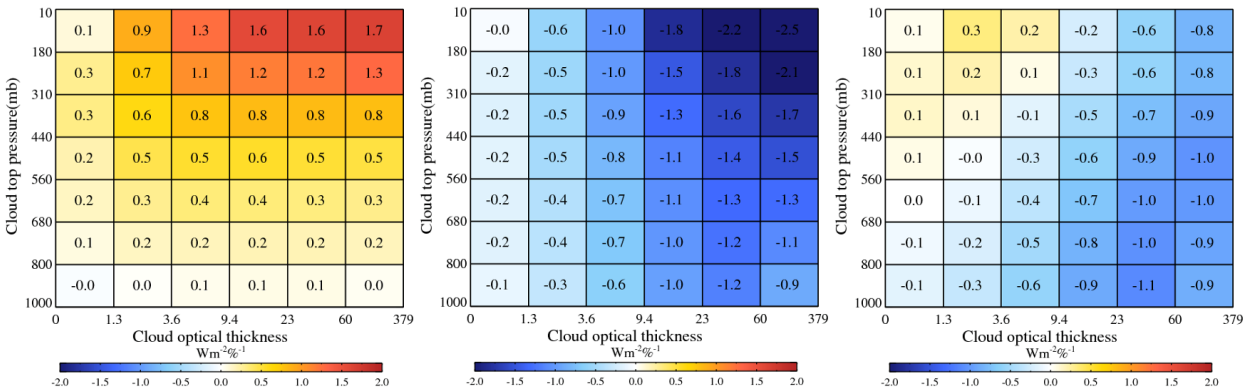

Figure 5-8. The 2010 FluxByCldTyp LW (left panel), SW (middle panel), and Net (right panel) global mean TOA flux radiative kernel in W $m^{-2}\%^{-1}$. Compare to Figure 1 in Zelinka et al. (2012).

5.6 FluxByCldTyp-Month Cloud-type Temporal Flux Consistency

The FBCT product can be used to monitor the regional cloud-type flux temporal variability. If the cloud algorithm were updated or the MODIS calibration drifted over the CERES record, it would be made manifest in the cloud-type monthly mean flux time series. Figure 5-9a shows the cloud-type SW fluxes as a function of increasing optical depths for a mid-layer cloud-type over the tropical western Pacific during July 2002 and December 2018. The cloud-type monthly SW flux variability increases with increasing optical depth and may have a seasonal component. The noisy monthly SW fluxes for the largest optical depth bin (brown line) are due to sporadic sampling. Figure 5-9b plots the LW fluxes according to decreasing pressure layer for a mid-thick optical depth bin. The slight increase in late 2016 of the lowest pressure layer LW fluxes (cyan line) shows when the cloud type had a cloud IR emissivity of 0.85, whereas for the rest of the time series the IR emissivity had an average value of 0.95. Note that the cloud-type SW and LW fluxes are stratified by cloud type and are not entwined. This demonstrates the robustness of the FBCT algorithm and the consistency of the CERES cloud properties.

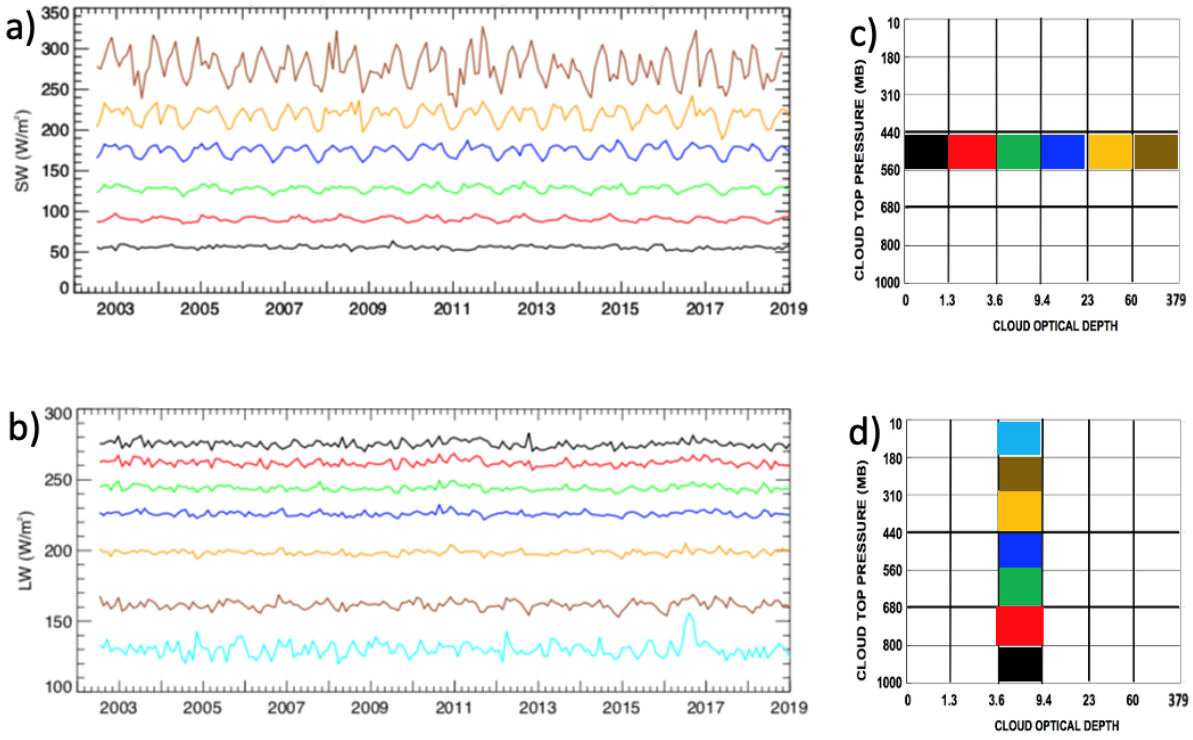

Figure 5-9. The cloud-type a) SW and b) LW monthly mean flux time series for the region located between 140° to 150° East and 0° to 10° North during July 2002 and December 2018. The c) SW cloud-types are ordered by increasing optical depth bins for a pressure layer between 560 to 440 hPa. The d) LW cloud-types are ordered by decreasing pressure bins for an optical depth between 3.6 and 9.4. The line colors in a) and b) correspond to the cloud effective pressure by optical depth cloud-type diagram to the right of each plot.

Figure 5-10a shows the 42 cloud-type mean SW fluxes over the same tropical western Pacific region between July 2002 and December 2018. The cloud-type SW fluxes are nearly stratified by optical depth bin. Figure 5-10b shows the corresponding cloud-type LW fluxes, which are layered by pressure level, except for the high thin cloud-types which have low cloud IR emissivities. The

cloud-types with the greatest frequency are in the 310 to 180 hPa bin (Figure 5-10c). The monthly cloud-type SW and LW variability is mostly within 6% and 3%, respectively. The greatest cloud-type SW flux variability are found over low but optically thick clouds and very thin cirrus (Figure 5-10d). It is remarkable that although many cloud-type bins have cloud fractions of less than 2% (Figure 5-10c), the mean cloud-type SW and LW fluxes show consistent patterns with little noise.

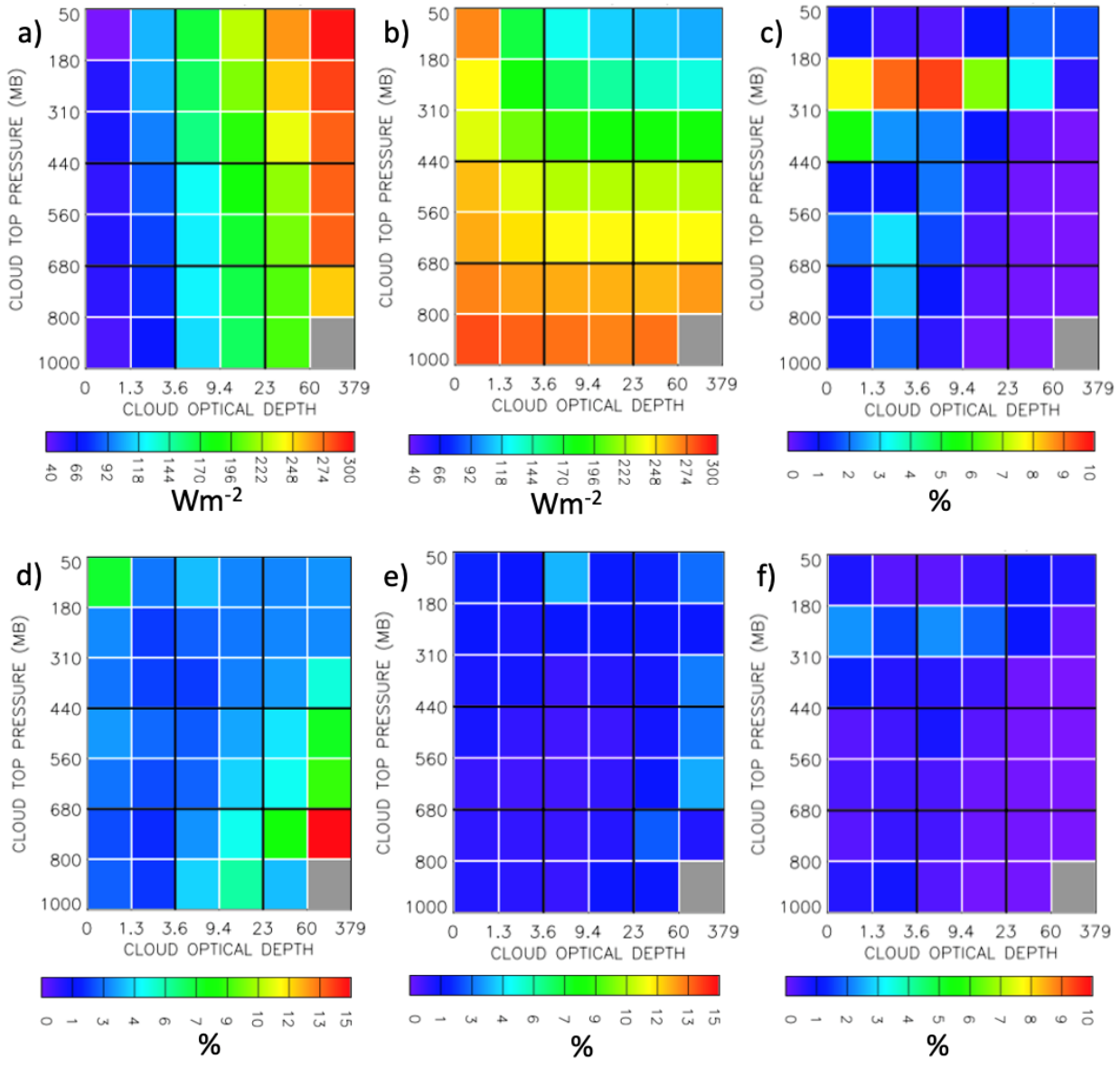

Figure 5-10. The cloud-type mean a) SW flux (W m^{-2}), b) LW flux (W m^{-2}), and c) cloud fraction (%) and associated monthly standard deviation of d) SW flux (%), e) LW flux (%), and f) cloud fraction for the region located between 140° to 150° East and 0° to 10° North. The mean is for the period July 2002 to December 2018.

6.0 References

Collins, W. D., P. J. Rasch, B. E. Eaton, B. V. Khattatov, J.-F. Lamarque, and C. S. Zender, 2001: Simulating aerosols using achemical transport model with assimilation of satellite aerosol retrievals: Methodology for INDOEX. *J. Geophys. Res*., **106**, 7313–7336, doi:10.1029/2000JD900507.

Doelling, D. R., N. G. Loeb, D. F. Keyes, M. L. Nordeen, D. Morstad, C. Nguyen, B. A. Wielicki, D. F. Young, and M. Sun, 2013: Geostationary enhanced temporal interpolation for CERES flux products. *J. Atmos. Oceanic Technol*., **30**, 1072-1090.

Doelling, D. R., M. Sun, L. T. Nguyen, M. L. Nordeen, C. O. Haney, D. F. Keyes, and P. E. Mlynczak, 2016: Advances in geostationary-derived longwave fluxes for the CERES Synoptic (SYN1deg) product, *J. Atmos. Oceanic Technol*. **33**, 503-521, doi: 10.1175/JTECH-D-15-0147.1.

Johnson, G. C., J. M. Lyman, and N. G. Loeb, 2016: Improving estimates of Earth's energy imbalance. *Nat. Clim. Change*, **6**, 639-640, doi:10.1038/nclimate3043.

Kato, S., and N. G. Loeb, 2003: Twilight irradiance reflected by the earth estimated from Clouds and the Earth's Radiant Energy System (CERES) measurements. *J. Climate*, **16**, 2646–2650.

Kato, S., and N. G. Loeb, 2005: Top-of-atmosphere shortwave broadband observed radiance and estimated irradiance over polar regions from Clouds and the Earth's Radiant Energy System (CERES) instruments on Terra, *J. Geophys. Res*., **110**, D07202, doi:10.1029/2004JD005308.

Kato, S., F. G. Rose, and T. P. Charlock, 2005: Computation of domain-averaged irradiance using satellite-derived cloud properties. *J. Atmos. Oceanic Technol.,* **22**, 146–164, doi: 10.1175/JTECH-1694.1.

Kopp, G., G. Lawrence, and G. Rottman, 2005: The Total Irradiance Monitor (TIM): Science Results, *Sol. Phys.*, **230**, 129-140.

Loeb, N. G., K. J. Priestley, D. P. Kratz, E. B. Geier, R. N. Green, B. A. Wielicki, P. O. R. Hinton, and S. K. Nolan, 2001: Determination of unfiltered radiances from the Clouds and the Earth's Radiant Energy System (CERES) instrument. *J. Appl. Meteor*., **40**, 822–835.

Loeb, N. G., N. M. Smith, S. Kato, W. F. Miller, S. K. Gupta, P. Minnis, and B. A. Wielicki, 2003: Angular distribution models for top-of-atmosphere radiative flux estimation from the Clouds and the Earth's Radiant Energy System instrument on the Tropical Rainfall Measuring Mission Satellite. Part I: Methodology. *J. Appl. Meteor*., **42**, 240–265.

Loeb, N. G., S. Kato, K. Loukachine, and N. M. Smith, 2005: Angular distribution models for top-of-atmosphere radiative flux estimation from the Clouds and the Earth's Radiant Energy System instrument on the Terra satellite. Part I: Methodology. *J. Atmos. Oceanic Technol.*, **22**, 338–351.

Loeb, N. G., S. Kato, K. Loukachine, and N. Manalo-Smith, 2007: Angular distribution models for top-of-atmosphere radiative flux estimation from the Clouds and the Earth's Radiant Energy System instrument on the Terra satellite. Part II: Validation. *J. Atmos. Oceanic Technol.*, **24**, 564–584.

Loeb, N. G., B. A. Wielicki, D. R. Doelling, G. L. Smith, D. F. Keyes, S. Kato, N. Manalo- Smith, T. Wong, 2009: Toward optimal closure of the Earth's top-of-atmosphere radiation budget. *J. Climate*, **22**, 748-766, doi:10.1175/2008JCLI2637.1.

Loeb, N. G., N. Manalo-Smith, W. Su, M. Shankar, and S. Thomas, 2016: CERES top-of-atmosphere earth radiation budget climate data record: accounting for in-orbit changes in instrument calibration. *Remote Sens.*, **8**(3), 182, doi:10.3390/rs8030182.

Loeb, N. G. et al., 2018: Clouds and the Earth's Radiant Energy System (CERES) Energy Balanced and Filled (EBAF) top-of-atmosphere (TOA) edition-4.0 data product, *J. Climate*, **31**, 895–918, doi:10.1175/JCLI-D-17-0208.1.

Loeb, N. G., F. G. Rose, S. Kato, D. A. Rutan, W. Su, H. Wang, D. R. Doelling, W. L. Smith, Jr., and A. Gettelman, 2020: Towards a consistent definition between satellite and model clear-sky radiative fluxes. *J. Climate*, **33**, 61-75, doi: 0.1175/JCLI-D-19-0381.1.

Loeb, N. G. and Doelling, D. R., 2020: CERES Energy Balanced and Filled (EBAF) from Afternoon-Only Satellite Orbits. *Remote Sens.*, **12**, 1280, doi:10.3390/rs12081280.

Minnis, P. et al., 2021: CERES MODIS cloud product retrievals for Edition 4, Part I: Algorithm Changes, *IEEE Trans. Geosci. Remote Sens.,* **59**, 2744-2780, doi: 10.1109/TGRS.2020.3008866.

Remer, L. A., and Coauthors, 2005: The MODIS aerosol algorithm, products, and validation. *J. Atmos. Sci.*, **62**, 947–973, doi:10.1175/JAS3385.1.

Rienecker, M., and Coauthors, 2008: The GEOS-5 data assimilation system—Documentation of versions 5.0.1, 5.1.0, and 5.2.0. M. J. Suarez, Ed., Tech. Rep. Series on Global Modeling and Data Assimilation, Vol. 27, NASA Tech. Memo. NASA/TM- 2008-104606, 101 pp.

Roemmich, D. et al., 2009: Argo: the challenge of continuing 10 years of progress. *Oceanography*, **22**, 46–55, doi:10.5670/oceanog.2009.65.

Su, W., J. Corbett, Z. A. Eitzen, and L. Liang, 2015a: Next-generation angular distribution models for top-of- atmosphere radiative flux calculation from the CERES instruments: Methodology. *Atmos. Meas. Tech*., **8**, 611–632.

Su, W., J. Corbett, Z. A. Eitzen, and L. Liang, 2015b: Next-generation angular distribution models for top-of- atmosphere radiative flux calculation from the CERES instruments: Validation. *Atmos. Meas. Tech*., **8**, 3297–3313.

Thomas, S., K. J. Priestley, N. Manalo-Smith, N. G. Loeb, P. C. Hess, M. Shankar, D. R. Walikainen, Z. P. Szewcyzk, R. S. Wilson, D. L. Cooper, 2010: Characterization of the Clouds and the Earth's Radiant Energy System (CERES) sensors on the Terra and Aqua spacecraft, Proc. SPIE, Earth Observing Systems XV, Vol. 7807, 780702, August 2010.

Trepte, Q. Z. et al., 2019: Global Cloud Detection for CERES Edition 4 Using Terra and Aqua MODIS Data, *IEEE Trans. Geosci. Remote Sens.*, doi:10.1109/TGRS.2019.2926620.

Wielicki, B. A., B. R. Barkstrom, E. F. Harrison, R. B. Lee III, G. L. Smith, and J. E. Cooper, 1996: Clouds and the Earth's Radiant Energy System (CERES): An Earth Observing System Experiment, *Bull. Amer. Meteor. Soc.*, **77**, 853-868, doi:10.1175/1520-0477(1996)077<0853:CATERE>2.0.CO;2.

Wu, A., X. Xiong, D.R. Doelling, D. Morstad, A. Angal, and R. Bhatt, 2013: Characterization of Terra and Aqua MODIS VIS, NIR and SWIR Spectral Bands Calibration Stability, *IEEE Trans. Geosci. Remote Sens*., **51**, 4330-4338, doi:10.1109/TGRS.2012.2226588

Yost, C. R., P. Minnis, S. Sun-Mack, Y. Chen, and W. L. Smith, 2021: CERES MODIS Cloud Product Retrievals for Edition 4, Part II: Comparisons to CloudSat and CALIPSO, *IEEE Trans. Geosci. Remote Sens.,* doi: 10.1109/TGRS.2020.3015155.

Zelinka, M. D., S. A. Klein, and D. L. Hartmann, 2012: Computing and partitioning cloud feedbacks using cloud property histograms. Part I: Cloud Radiative Kernels, *J. Climate*, **25**, 3736–3754.

7.0 Expected Reprocessing

There are no plans to reprocess the FluxByCldTyp Ed4A record until the CERES Edition 5 suite of data products is available. Any updates to the CERES FluxByCldTyp products will be available for subsetting/visualization/ordering at: https://ceres.larc.nasa.gov/data/.

8.0 Attribution

When referring to the CERES FluxByCldTyp product, please include the product and data set version as: "CERES FluxByCldTyp Ed4A"

The CERES Team has put forth considerable effort to remove major errors and to verify the quality and accuracy of this data. Please provide a reference to the following papers when you publish scientific results with the CERES FluxByCldTyp Edition4A:

Wielicki, B. A., B. R. Barkstrom, E. F. Harrison, R. B. Lee III, G. L. Smith, and J. E. Cooper, 1996: Clouds and the Earth's Radiant Energy System (CERES): An Earth Observing System Experiment, *Bull. Amer. Meteor. Soc.*, **77**, 853-868.

Sun, M., D. R. Doelling, J. Wilkins, …, 2020: Clouds and the Earth's Radiant Energy System (CERES) FluxByCldTyp Top-of-Atmosphere (TOA) Data Product, in preparation.

The CERES data products now have DOIs. To cite the data in a publication, use this format:

CERES Science Team, Hampton, VA, USA: NASA Atmospheric Science Data Center (ASDC), Accessed <**author citing data inserts date here**> at doi: (appropriate product)

For FluxByCldTyp-Day:
10.5067/Terra-Aqua/CERES/FLUXBYCLDTYP-DAY_L3.004A

For FluxByCldTyp-Month:
10.5067/Terra-Aqua/CERES/FLUXBYCLDTYP-MONTH_L3.004A

When Langley ASDC data are used in a publication, we request the following acknowledgment be included: "These data were obtained from the NASA Langley Research Center Atmospheric Science Data Center."

The Langley ASDC requests a reprint of any published papers or reports or a brief description of other uses (e.g., posters, oral presentations, etc.) of data that we have distributed. This will help us determine the use of data that we distribute, which is helpful in optimizing product development. It also helps us to keep our product related references current.

When CERES data obtained via the CERES web site are used in a publication, we request the following acknowledgment be included: "These data were obtained from the NASA Langley Research Center CERES ordering tool at https://ceres.larc.nasa.gov/data/."

9.0 Feedback and Questions

For questions or comments on this CERES FluxByCldTyp-Day/Month Data Quality Summary, contact the User and Data Services staff at the Atmospheric Science Data Center.

For questions about the CERES subsetting/visualization/ordering tool at https://ceres.larc.nasa.gov/data/, please email LaRC-CERES-Help@mail.nasa.gov.

10.0 Document Revision Record

The Document Revision Record contains information pertaining to approved document changes. The table lists the Version Number, the date of the last revision, a short description of the revision, and the revised sections.

Document Revision Record

Version Number	Date	Description of Revision	Section(s) Affected
V1	08/09/2021	• Existing document put in version control.	All
V2	02/03/2022	• Added bullet regarding correction to daily albedo calculation.	Section 3